Cellular and Molecular Bioengineering, Vol. 2, No. 2, June 2009 (© 2009) pp. 207 217
DOI: 10.1007/s12195-009-0063-9

Dynamics of Microvillus Extension and Tether Formation in Rolling Leukocytes

MARIA K. POSPIESZALSKA and KLAUS LEY

Division of Inflammation Biology, La Jolla Institute for Allergy and Immunology, 9420 Athena Circle, La Jolla, CA 92037, USA

(Received 23 March 2009; accepted 15 May 2009; published online 11 June 2009)

Abstract—P-selectin glycoprotein ligand-1 (PSGL-1) binding to P-selectin mediates leukocyte rolling under conditions of flow. In human neutrophils, a type of leukocyte belonging to the innate immune system, PSGL-1 molecules are located on the neutrophil's surface ruffles, called microvilli. Each newly formed P-selectin–PSGL-1 bond can become load bearing, imposing on its microvillus a pulling force that deforms the microvillus. Depending on the magnitude of the bond force, a microvillus can be extended, or a thin membrane cylinder (a tether) can be formed at the tip of the microvillus. Here we propose a Kelvin–Voigt viscoelastic material as an improved model for microvillus extension. Using a modified version of our Event-Tracking Model of Adhesion (ETMA), we demonstrate how P-selectin–PSGL-1 load-bearing bonds shape microvillus deformation during neutrophil rolling at low shear (wall shear rate of 50 s^{-1}, P-selectin site density of 150 molecules μm^{-2}). We also discuss the impact of microvillus deformability on neutrophil rolling. We find that the average microvillus extension constitutes 65% of the total microvillus–tether complex extension, and that the rolling neutrophil may never fully rest. A quantitative comparison with the corresponding non-deformable microvilli case supports a concept that the ability of the microvillus to deform stabilizes cell rolling.

Keywords—Leukocyte rolling, Neutrophil, P-selectin, PSGL-1, Microvillus deformation, Microvillus elongation, Microvillus tether, Modeling of cell rolling, Kelvin–Voigt, ETMA.

INTRODUCTION

Leukocytes are immune cells involved in host defense. To reach sites of inflammation, leukocytes roll along the vascular endothelium (that lines the interior surface of blood vessels) by a series of molecular bonds between the leukocyte and the endothelium that rapidly form and dissociate. The bonds work against the forces exerted on the leukocyte by the flowing blood, such that each rolling leukocyte travels at a fraction of its free-flow velocity.[2]

Most leukocyte rolling is mediated by P-selectin glycoprotein ligand-1 (PSGL-1 or CD162) binding to P-selectin (CD62P) expressed on the inflammation-activated endothelium (Fig. 1). Human neutrophils, a type of leukocyte belonging to the innate immune system, have surface ruffles, called microvilli.[5,11] The PSGL-1 molecules are present on the microvilli tips (Fig. 1).[5] Most newly created P-selectin–PSGL-1 bonds bear no load initially, and some dissociate before becoming load bearing.[23] Because of the cell's motion, bonds can become load bearing (i.e., positioned in a straight line with the microvillus and stretched beyond the equilibrium length, as seen in Fig. 1), imposing on the microvillus a pulling force which make the cell roll more slowly or even stop.

It has been observed experimentally that the bond force causes microvillus deformation. Micropipette experiments of Shao *et al.*[29] reveal that low forces (<34 pN) cause the microvillus to extend, while high forces (>61 pN) cause a thin membrane cylinder (a tether) to be formed at the tip of the microvillus, although the microvillus length does not change. When the force is between 34 and 61 pN, the degree of association between membrane and cytoskeleton in individual microvilli dictates whether microvillus extension or tether formation occurs.[29] Evidence for tether formation was also found by high-speed, high-resolution videomicroscopy[28] at a wall shear rate of 150 s^{-1} and by differential interference contrast videomicroscopy[25] at a wall shear rate of 200 s^{-1}, although the resolution of these light microscopy-based methods is insufficient to resolve ~50 nm thin tether structures. The high-speed, high-resolution videomicroscopy method fails to notice microvillus tether formation at wall shear rates of 50 s^{-1} and below.[28] Our modeling, conducted at a wall shear rate of 50 s^{-1}, shows both microvillus deformation and tether formation that may not be observable with current experimental techniques.

Address correspondence to Klaus Ley, Division of Inflammation Biology, La Jolla Institute for Allergy and Immunology, 9420 Athena Circle, La Jolla, CA 92037, USA. Electronic mail: mpospieszalska@liai.org, klaus@liai.org

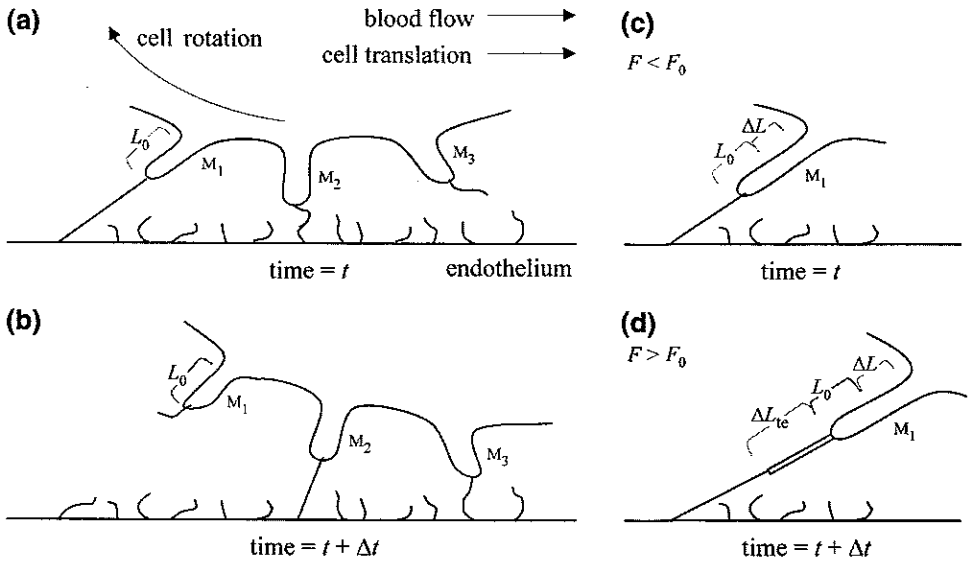

FIGURE 1. Conceptual model of non-deformable (left, a–b) and deformable (right, c–d) microvilli in the cell-substrate contact area. For simplicity only one ligand per microvillus tip is shown. L_0, ΔL, F, and F_0 are the microvillus equilibrium length, extension, bond force, and threshold bond force, respectively. ΔL_{te} is the tether extension. (a–b) The microvillus length is assumed to be fixed, but the microvillus can pivot about its base. At time t microvillus M_1 has a load-bearing bond, microvillus M_2 has a bond bearing no load, and microvillus M_3 has no bond. At time $t + \Delta t$ the bond of M_1 is already broken, the bond of M_2 is load-bearing, and the newly formed bond of M_3 has no load yet. (c–d) Microvilli are allowed to extend and form tethers. If $F < F_0$ at time t, then microvillus M_1 will be longer than in (a). If $F > F_0$ at time $t + \Delta t$, then most likely the bond of microvillus M_1 will still exist (compare d with b), the microvillus will be longer than in (c), and a tether will be developed.

There has been a substantial effort to model microvillus deformation. Khismatullin and Truskey[14] assume a spring model for microvillus extension. To simulate cell rolling, Shao *et al.*[29] propose a spring model for microvillus extension and a viscous model for microvillus tether formation. The same method is adopted by Caputo and Hammer[6] to model microvillus deformation in cell rolling using Adhesion Dynamics (AD), and by Pawar *et al.*[22] to model cell deformability in cell rolling using a finite element Immersed Boundary Method (IBM). Here, we use the existing model for microvillus tether formation and propose a Kelvin–Voigt (also known as Kelvin–Voight) viscoelastic material as an improved model for microvillus extension. The proposed model is in good agreement with the experimental data of Shao *et al.*[29] Using a modified version of our Event-Tracking Model of Adhesion (ETMA),[23] we conducted multiple simulations of neutrophil rolling. By directly comparing the microvillus deformation process with the lifetimes of load-bearing bonds of that microvillus, we demonstrate how P-selectin–PSGL-1 load-bearing bonds shape microvillus deformation during neutrophil rolling. Based on the improved model for microvillus extension, our study was intended to identify the patterns of microvillus deformation, distinguish the contributions of microvillus extension and tether formation, study the impact of deformable microvilli on leukocyte rolling, and compare our modeling results with experimental work studying human neutrophils in a flow chamber.[20]

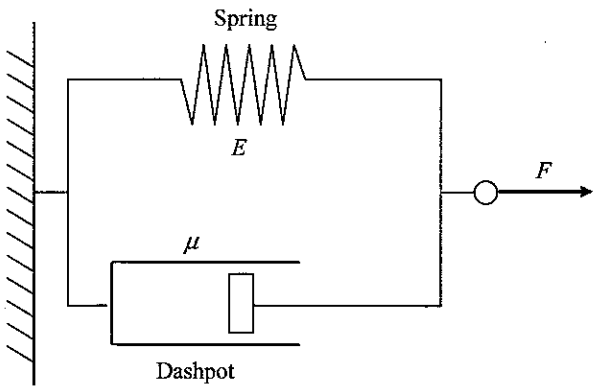

FIGURE 2. Schematic representation of a Kelvin–Voigt element. It is composed of a Hookean elastic spring of elastic modulus E and a Newtonian damper (represented here by a dashpot) of viscosity μ, connected in parallel.

MATERIALS AND METHODS

Model of Microvillus Deformation

The micropipette experiments of Shao *et al.*[29] demonstrate that under a low bond force, not greater than 34 pN, the microvillus extends. For a fixed suction pressure imposed in a micropipette on a neutrophil bound to a bead (Shao *et al.*,[29] Fig. 2), the

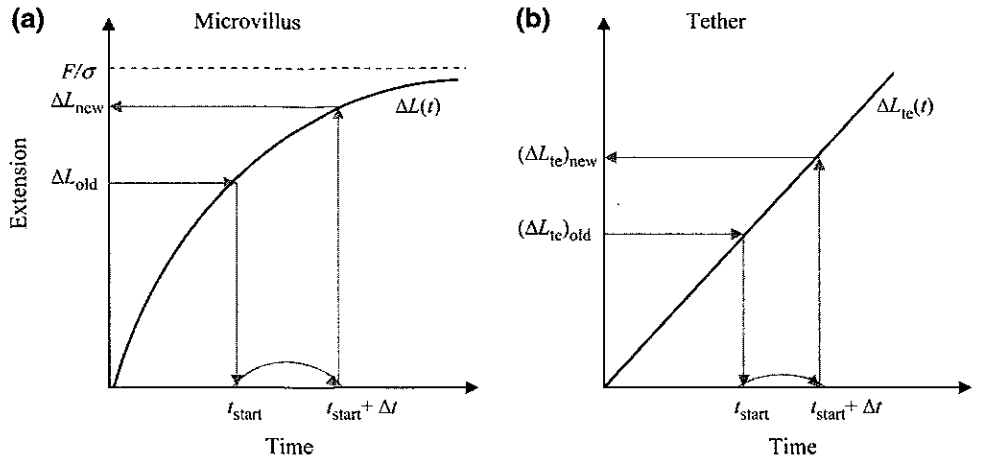

FIGURE 3. Illustration for calculations of microvillus extension (a) and microvillus tether extension (b), for time step Δt. ΔL_{old} [$(\Delta L_{te})_{old}$] is the microvillus [tether] extension at the beginning of the time step, and ΔL_{new} [$(\Delta L_{te})_{new}$] is the microvillus [tether] extension at the end of the time step. $\Delta L(t) = (F/\sigma)\{1 - \exp[-t/(\eta/\sigma)]\}$ and $\Delta L_{te}(t) = [(F - F_0)/\eta_{te}]t$, where F, F_0, σ, and η are the microvillus bond force (assumed to be constant for the time step), threshold force, spring constant and effective viscosity, respectively. Symbol η_{te} denotes the effective viscosity of the microvillus tether.

microvillus extension is an increasing function of time approaching a horizontal asymptote (Shao *et al.*,[29] Fig. 3a). The microvillus needs some time (about 3 s for a suction pressure of 0.5 pN μm^{-2}, corresponding to a force of 34 pN) to reach its approximately final length. The authors report that an ad-hoc "intuitive formula" for the microvillus total length, L, at time t matches their experimental data well:

$$L(t) = L_\infty - (L_\infty - L_0)\exp(-t/t_c), \qquad (1)$$

where L_∞ is the asymptotic length that the microvillus approaches as $t \to \infty$, L_0 is the equilibrium length of the microvillus, and t_c is what the authors call the characteristic time of extension. Interestingly, t_c is independent of the bond force, suggesting that it is probably an inherent characteristic that may be determined by the shape and other properties of microvilli.

Here, we propose and use a Kelvin–Voigt viscoelastic material as a model for microvillus extension. The Kelvin–Voigt element is composed of a Hookean elastic spring and a Newtonian damper, connected in parallel. It can be represented by a spring of elastic modulus E and a dashpot (a piston moving in a liquid) of viscosity μ, as seen in Fig. 2. Let $\sigma = EA_0/L_0$ and $\eta = \mu A_0/L_0$, where A_0 is the microvillus cross-section, and σ and η represent, respectively, the microvillus spring constant and its effective viscosity. At any time t, constant force F acting on the Kelvin–Voigt element has spring and damper components as follows:

$$F = \sigma[\Delta L(t)] + \eta[dL(t)/dt], \qquad (2)$$

where $\Delta L(t) = L(t) - L_0$ is the total extension of the microvillus at time t. The solution to differential Eq. (1), with the initial condition $\Delta L(0) = 0$, yields the following formula for the microvillus extension at time t:

$$\Delta L(t) = (F/\sigma)\{1 - \exp[-t/(\eta/\sigma)]\} \qquad (3)$$

Equation (3) is valid as long as force F is applied. Extension function $\Delta L(t)$ increases to asymptotically approach

$$\Delta L(\infty) = L_\infty - L_0 = F/\sigma, \qquad (4)$$

where $\Delta L(\infty)$ approximates the length of the microvillus if constant bond force F acts for a sufficiently long time (Fig. 3a). Extension $\Delta L(t)$, given by Eq. (3), is in good agreement with the experimental data of Shao *et al.*,[29] since substituting F/σ in Eq. (3) with $(L_\infty - L_0)$ yields Eq. (1) with $t_c = \eta/\sigma = \mu/E$. This implies that the characteristic time of extension introduced by Shao *et al.*[29] is the same as Kelvin–Voigt material parameter $\tau = \mu/E$, called the relaxation time.

The micropipette experiments of Shao *et al.*[29] demonstrate that under a high bond force, F, greater than 61 pN, the microvillus does not extend but grows a tether at a constant rate (Shao *et al.*,[29] Fig. 3b). We therefore view the microvillus tether as a dashpot described by the following equations[29]:

$$F - F_0 = \eta_{te}[dL_{te}(t)/dt] \qquad (5)$$

and

$$\Delta L_{te}(t) = [(F - F_0)/\eta_{te}]t, \qquad (6)$$

where $L_{te}(t)$ is the length of the tether at time t, $\Delta L_{te}(t)$ is the total tether extension at time t, η_{te} is the tether effective viscosity, and F_0 is called the threshold bond force and represents the force at which a given

microvillus stops extending and starts developing a tether (Fig. 3b).

Model of Rolling for Cells with Deformable Microvilli

We use a modified version of our Event-Tracking Model of Adhesion (ETMA)[23] to simulate the rolling of cells with deformable microvilli. In the original version of ETMA the microvilli can bend and they can pivot at their base, but they cannot deform lengthwise. The neutrophil is modeled as a spherical body, with microvilli distributed randomly on its surface. The PSGL-1 molecules (ligands) are present on the microvilli tips. P-selectin molecules (receptors) are randomly distributed on the substratum. Because of fluid flow, the neutrophil translates and rotates, as indicated in Fig. 1a. Bonds form and dissociate in the contact area depending on the separation distance between receptors and ligands, under probabilistic rules governed by the reaction rates of Dembo.[8] The bond force is calculated according to the Hookean spring model. The cell's instantaneous velocities, translational, rotational, and perpendicular to the substratum, are calculated from current bond, fluid, gravitational, and repulsive forces acting on the cell. The modeling progresses by varying time steps dictated by the time intervals between consecutive bond formation/dissociation events as described in Pospieszalska *et al.*[23] At every time step, the positions of the microvilli tips, bonds, free ligands, and free receptors in the contact zone are updated. In the modified version of ETMA used here, the updates reflect the changes in the microvillus and tether lengths (see below and Figs. 1c and 1d).

The threshold bond force, F_0, separating microvillus extension and tether regimes, is different for different microvilli. It has been experimentally established[29] that 34 pN $< F_0 <$ 61 pN. Shao *et al.*[29] and others[6,22] assume the same threshold force of $F_0 = 45$ pN for all microvilli. To better cover the range of possible threshold forces, we select the threshold bond force independently for each microvillus from the normal distribution with a mean of 47.5 pN and seven standard deviations fitting segment ⟨34 pN, 61 pN⟩. If the selection is $F_0 <$ 34 pN [$F_0 >$ 61 pN], then we reset that $F_0 = 34$ pN [$F_0 = 61$ pN].

The bond force on a microvillus constantly changes as the cell rolls. This means that for every time step, a slightly different curve $\Delta L(t)$ or $\Delta L_{te}(t)$ is valid than in the previous time step. Knowing the microvillus extension at the end of the previous time step, ΔL_{old}, and assuming that bond force F ($F < F_0$) will be valid for the next Δt time interval, Eq. (3) with $\Delta L(t) = \Delta L_{old}$ is solved for $t = t_{start}$. The new microvillus extension, ΔL_{new}, that will be achieved at the end of the Δt time interval is calculated from Eq. (3) as $\Delta L_{new} = \Delta L(t_{start} + \Delta t)$. The above calculations (illustrated in Fig. 3a) are carried out if $\Delta L_{old} < F/\sigma$, which is typically the case. In rare cases when $\Delta L_{old} > F/\sigma$, we approximate the new microvillus extension with $\Delta L_{new} = F/\sigma$. Similarly, for $F > F_0$ we calculate $(\Delta L_{te})_{new}$ from Eq. (6) [no conditions on $(\Delta L_{te})_{old}$, illustrated in Fig. 3b].

If a microvillus is attached to the substrate by just one load-bearing bond, it will first extend and then develop a tether because of the increasing bond force as the cell rolls, as illustrated in Figs. 1c and 1d. The process ends when the bond dissociates. A microvillus with multiple load-bearing bonds may experience an instantaneous decrease in its bond force (the microvillus bond force is due to all the load-bearing bonds of this microvillus) when one of the microvillus's load-bearing bonds breaks while its other load-bearing bonds are still in place. If the decreased bond force falls below the threshold force for that microvillus, we assume that the microvillus adjusts its length accordingly, while the length of its tether does not change. If the decreased bond force is still above the threshold force for the microvillus, the tether continues growing, although at a slower rate. In addition, we assume that the microvillus tether snaps back fully after all microvillus bonds break and the microvillus leaves the contact area on the cell's trailing side.[28] Through this mechanism, all tethers have retracted and all microvilli have returned to their resting length when they enter the contact area again on the cell's leading side. Rare cases in which the tether breaks off the microvillus and is left behind on the substratum are not modeled.

RESULTS

Our analyses were conducted for human neutrophils rolling on a P-selectin-coated substrate (150 molecules μm^{-2}) at a wall shear rate of 50 s^{-1}, under the established physiological and biophysical parameters listed in Table 1. The simulations were performed at a time resolution of 10^{-4} s or better to generate Figs. 4–6, and at a time resolution of 10^{-5} s or better to generate quantitative descriptions. Shorter time steps did not significantly alter the results (data not shown).

Case Study

The series of three diagrams in Fig. 4 shows the deformation history of all microvilli which became stressed by P-selectin–PSGL-1 load-bearing bonds during the first 1.25 s of rolling, for one neutrophil in the study (also referred to as the sample cell). The diagrams show the length of the microvillus–tether

TABLE 1. Model parameters.

Parameter (symbol)	Value	Reference
Cell radius	3.8 μm	27
Cell density	1.077 g cm^{-3}	31
Microvillus length (L_0)	200 nm	9
Microvillus radius	50 nm	9
Microvilli per cell	941	5
PSGL-1 length	50 nm	16
PSGL-1 dimers per microvillus	8	19
P-selectin length	40 nm	30
P-selectin site density	150 molecules μm^{-2}	18
Suspending medium viscosity	0.01 g cm^{-1} s^{-1}	10
Suspending medium density	1.025 g cm^{-3}	
Wall shear rate	50 s^{-1}	
Temperature	290 °K	
Glycocalyx repulsion constant	10 pN	3
Glycocalyx effective thickness	15 nm	3
Bond bound state spring constant	1 dyn cm^{-1}	8
Bond transition state spring constant	0.98 dyn cm^{-1}	8
Equilibrium bond length	70 nm	21
Equilibrium forward reaction rate	1 s^{-1}	4,17
Equilibrium reverse reaction rate	1 s^{-1}	4,17
Microvillus spring constant (σ)	43 pN μm^{-1}	29
Microvillus effective viscosity (η)	30.1 pN s μm^{-1}	29
Tether effective viscosity (η_{te})	11 pN s μm^{-1}	29

complex as a function of time. The curves represent scatter plot data. The equilibrium length of the modeled microvilli is 200 nm; therefore, each curve starts at a minimum length of 200 nm, followed by a combination of black segments when the microvillus extends and red segments when the microvillus tether develops. The curve ends when the last load-bearing bond of the microvillus breaks. Many microvilli, especially those loaded soon after the first contact of the cell with the substrate, were attached to the substrate by one load-bearing bond only. Some microvilli (marked with arrows) developed two, three, or four load-bearing bonds with overlapping lifetimes. The number of load-bearing bonds and their overlapping pattern are indicated by the inserts. In general, a microvillus with a higher number of load-bearing bonds develops a longer extension/tether.

Figure 5a shows the deformation history for the microvillus marked with one asterisk in Fig. 4c. This microvillus's threshold force is $F_0 = 49.8$ pN. The microvillus developed three load-bearing bonds, marked B1, B2, and B3. Their durations are represented by the green horizontal bars. A combined force of the three bonds (illustrated in Fig. 5a) extended the microvillus–tether complex by 37 nm, mostly because of microvillus extension. Figure 5b shows the deformation history of the microvillus marked with two asterisks in Fig. 4c. This microvillus developed four load-bearing bonds that generated a microvillus-tether complex extension of 61 nm, mostly because of tether formation. Red, almost horizontal parts of the curve indicate a very slow rate of tether extension, caused by bond forces [of approximately $F = 48.5106$ pN (left) and $F = 48.5107$ pN (right)] barely exceeding the threshold force, for this microvillus, of $F_0 = 48.5105$ pN. The arrows point to episodes in microvillus extension which are too short to be visible in the diagram as black segments. In addition, black, almost horizontal parts in length curves have been observed (data not shown), each indicating a very slow rate of microvillus extension caused by a bond force barely below the threshold force at which that microvillus would form a tether. As seen in Figs. 5a and 5b, periods of time in which the number of existing load-bearing bonds is locally maximized promote high rates of tether formation. Figure 5c shows the bond force acting on the microvillus discussed in Fig. 5b, which complements well the microvillus deformation process. The dashed, horizontal line marks the microvillus threshold force. In general, the microvillus bond force decreases as the microvillus/tether length increases. A longer microvillus–tether complex makes its load-bearing bonds shorter, which, in turn, according to the Hookean spring model, reduces the force on each bond.

The displacement, microvillus deformation and translational velocity of the sample cell rolling for about 2.75 s are shown in Figs. 6a, 6b, and 6c, respectively. The first, one-bond, short-time-loaded microvilli cause only a small reduction in cell velocity;

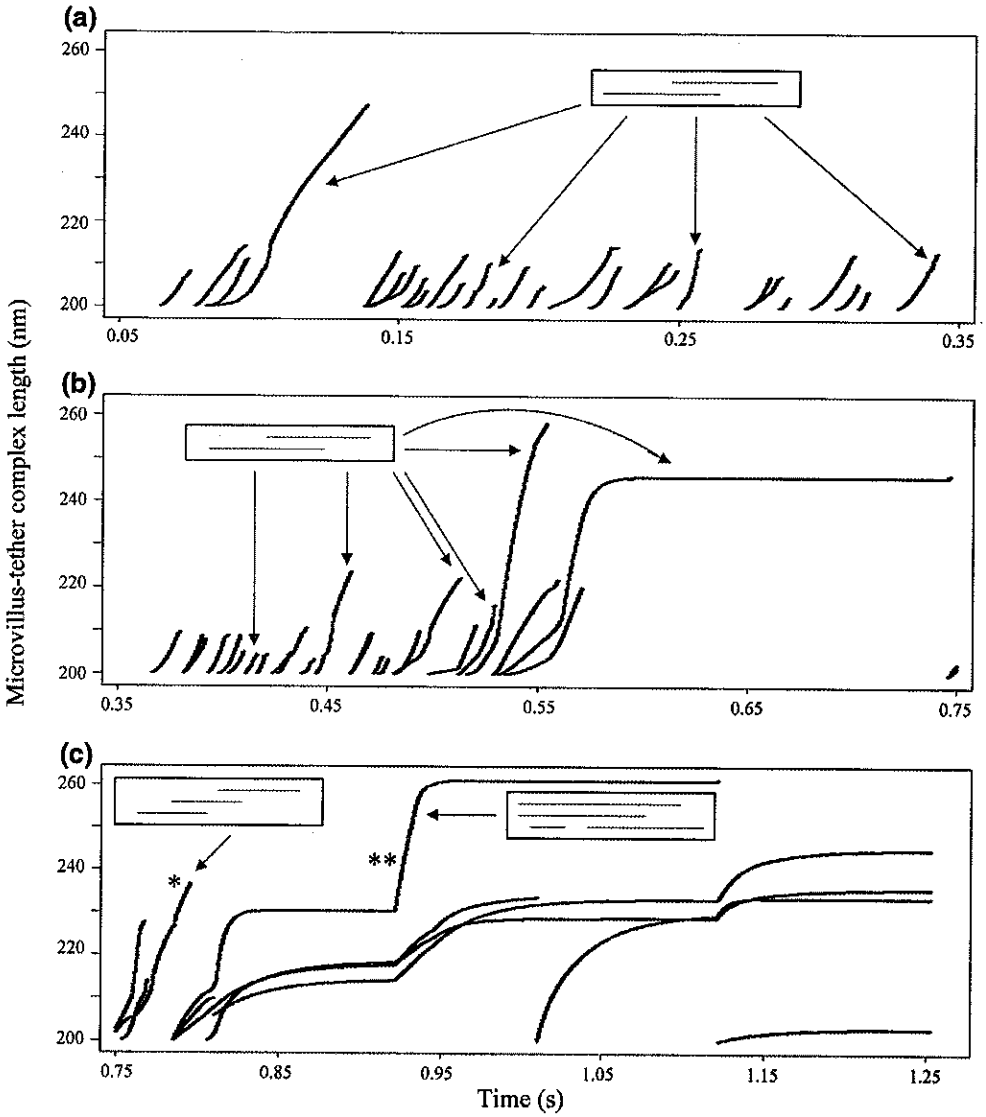

FIGURE 4. Deformation history for all microvilli that became stressed by P-selectin–PSGL-1 load-bearing bonds during the first 1.25 s the sample cell rolled. The equilibrium length of each microvillus is 200 nm. (a) $t < 0.35$ s, (b) $0.35 \text{ s} < t < 0.75$ s, and (c) $0.75 < t < 1.25$. The black segments represent periods of microvillus extension, and the red segments periods of tether extension. The arrows point to the curves representing the microvilli deformed by more than one load-bearing bond. The inserts indicate the number of load-bearing bonds and their overlapping pattern. The horizontal green bars symbolically illustrate the bond duration. Vertical overlapping of two bars indicates that two load-bearing bonds of a microvillus coexist for a period of time.

however, the reduction is sufficient to allow for multiple bonds to be formed on the next microvilli. The cell in turn rolls more slowly and shows periods of very little or no motion. One surprising behavior of the cell that generated the velocities seen in the dashed boxes was further investigated. The small changes in velocity are not seen if the velocity data are filtered to 60 frames per second, a time resolution commonly used in experiments (Fig. 6d). A closer look at 0.15 s of the velocity profile (Figs. 6e and 6f) shows that the cell, while almost resting, makes steps forward that are invisible to an experimenter. This points to the fact that there is no absolute rest for a rolling cell with deformable microvilli. The cell's motionless appearance is caused by the bond forces almost balancing the fluid forces. The presence of the bond forces causes the affected microvilli to deform. Microvillus/tether elongation, and therefore bond force reduction, are continuous processes. Therefore, the cell is never really at rest, though its smallest steps may very well not be noted both, experimentally and in modeling (as in Fig. 6b near $t = 1$ s). The small spikes separated by spaces, seen in Fig. 6d, only approximately represent cell movement because direct

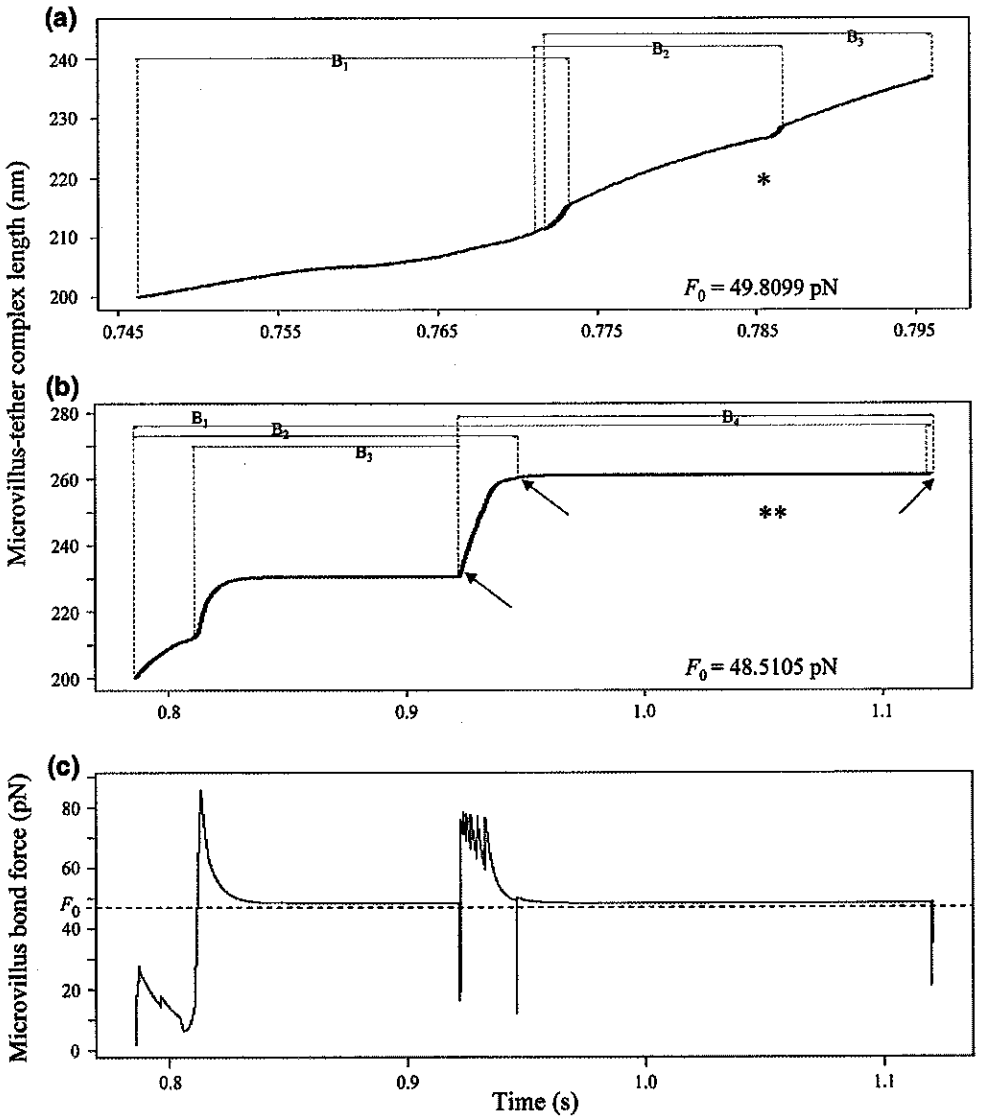

FIGURE 5. (a) Deformation history for the microvillus marked with one asterisk in Fig. 4c. The lifetimes of three load-bearing bonds, B1, B2, and B3, developed by the microvillus, are represented by the green horizontal bars. F_0 is the microvillus's threshold force. (b) Similarly, the deformation history for the microvillus marked with two asterisks in Fig. 4c. The arrows point to episodes in microvillus extension which are too short to be visible in the diagram as black segments. (c) Bond force acting on the microvillus discussed in (b). The dashed, horizontal line marks the microvillus threshold force.

modeling is discrete, progressing by small time steps, never ideally continuous.

Quantitative Description

In order to obtain high-confidence numerical characteristics for the cell rolling process, we conducted ten simulations for ten different cells with deformable microvilli. Each simulation generated 5–6 s of cell rolling. The resulting data were compared with our existing data for cells with non-deformable microvilli rolling under the same conditions.[23] 95% confidence intervals for the mean values of the key variables in the cell rolling process are given in Table 2. The intervals are based on 10-element samples for cells with deformable microvilli, and 20-element samples for cells with non-deformable microvilli. The obtained quantitative data imply an interval of 235.7 ± 3 nm for the mean final length of the microvillus–tether complex; however, deformation for some microvilli may be much more extensive. A 10-s rolling period of one cell yields 51.2% and 71.2% of microvillus–tether complexes reaching final lengths below 210 and 230 nm, respectively. The remaining data is almost uniformly distributed with the three longest complexes being 354, 355, and 368 nm long. The length of the longest

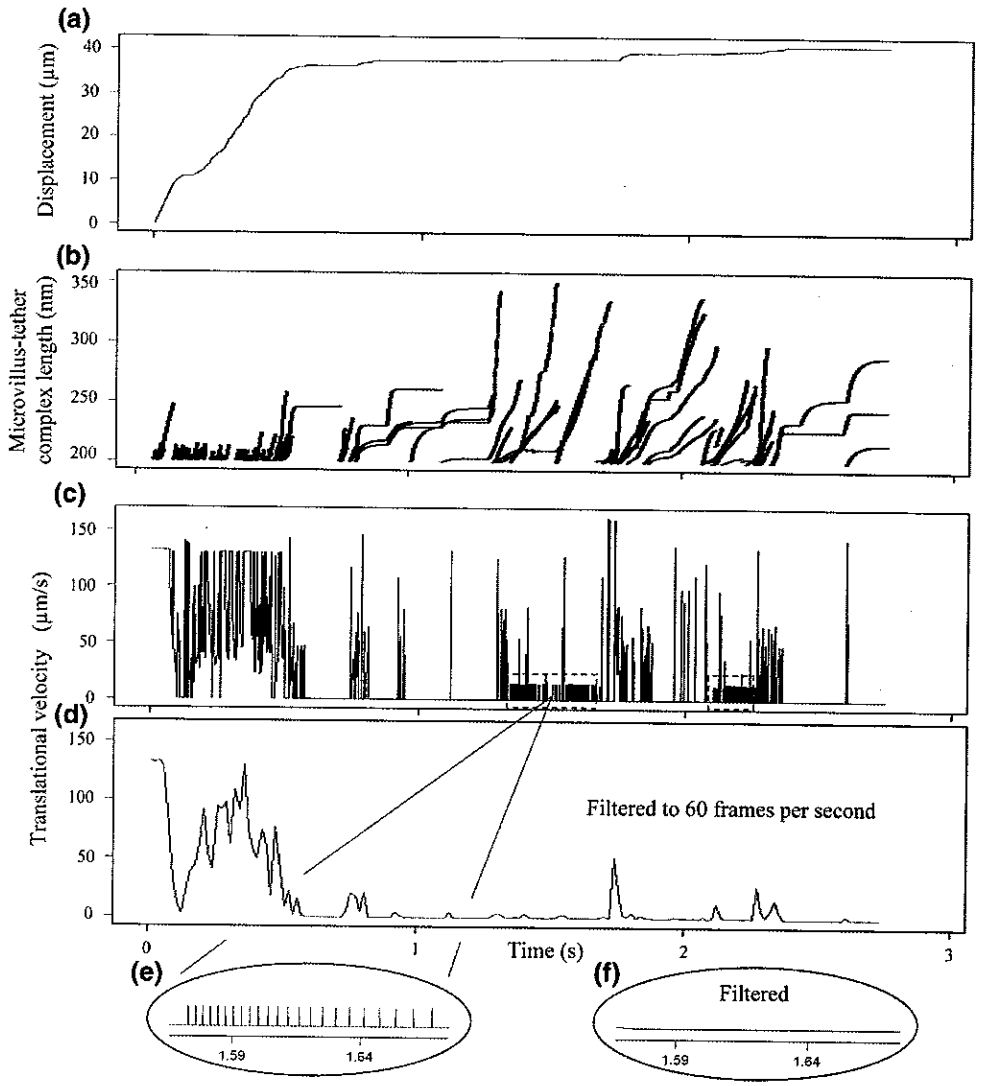

FIGURE 6. Displacement (a), deformation history (b), translational velocity not filtered (c), and filtered to 60 frames per second (d), for all microvilli that became stressed by P-selectin–PSGL-1 load-bearing bonds during the first 1.25 s the sample cell rolled. (e) High resolution of a 0.15-s segment of data in (c). (f) Data in (e) filtered to 60 frames per second.

TABLE 2. 95% confidence intervals for the mean values.

Variable (unit)	Cells with non-deformable microvilli	Cells with deformable microvilli
Translational velocity (μm s^{-1})	3.42 ± 0.51	2.23 ± 1.17
Cell body to substrate separation distance (nm)	164.5 ± 0.5	164.6 ± 0.56
Total number of bonds	16.6 ± 0.8	19.9 ± 1.73
Total number of load-bearing bonds	3.7 ± 0.2	3.75 ± 0.21
Fraction of bonds that become load-bearing (%)	69 ± 2.5	55.2 ± 3.6
Bond lifetime (s)	0.39 ± 0.03	0.5 ± 0.04
Lifetime of bonds that become load-bearing (s)	0.44 ± 0.04	0.62 ± 0.07
Duration of their load-bearing stage (s)	0.13 ± 0.01	0.2 ± 0.02
Number of load-bearing microvilli	n.d.	2.54 ± 0.19
Force on microvillus when its last bond breaks (pN)	n.d.	55 ± 2.3
Microvillus final length (nm)	200	223.2 ± 2.3
Tether final length (nm)	0	12.5 ± 2.2
Total deformation time of microvillus–tether complex (s)	0	0.36 ± 0.06
Microvillus growth rate (nm s^{-1})	0	68 ± 13.5
Tether growth rate (nm s^{-1})	0	35.3 ± 4.3

complex constitutes 184% of the microvillus equilibrium length.

DISCUSSION

Kelvin–Voigt models have been successfully used to capture certain mechanical properties occurring in cells. Ragsdale *et al.*[24] reported that the cytoplasm of a Swiss 3T3 fibroblast, stressed by a neighboring cell through adherens junctions, responds as a Kelvin–Voigt viscoelastic material. Kumar *et al.*[15] find that viscoelastic properties of a single stress fiber in its normal physiological context within a living cell can be represented by a Kelvin–Voigt element. In this work we demonstrated that deformation of a Kelvin–Voigt viscoelastic material is also an accurate representation of microvillus extension, in agreement with the experimental data of Shao *et al.*[29] Our finding is both consistent with and supports the modeling approach of Ragsdale *et al.*[24] The incorporation of the Kelvin–Voigt model into ETMA allowed for more accurate modeling of microvillus deformation in cell rolling than the previous modeling efforts.[6,22,29] Under the conditions studied (Table 1), we conducted analyses of the factors shaping microvillus deformation, presented the first detailed examples of how microvilli deform, derived quantitative characteristics of cell rolling for cells with deformable microvilli, comparing them to the corresponding non-deformable microvilli case, and numerically described microvillus and tether properties in rolling cells.

Two competing trends shape the rolling of cells with deformable microvilli. On the one hand, elongation of a microvillus–tether complex during cell rolling makes the involved load-bearing bonds slightly shorter than in the corresponding non-deformable microvilli case. Shorter bonds yield lower bond forces resulting in higher cell translational velocities. On the other hand, shorter bonds generally live longer, resulting in lower cell translational velocities. Our quantitative data indicate that under the conditions studied the latter is dominant, since introducing deformable microvilli reduces the mean translational velocity of the cell. Interestingly, the deformability of microvilli does not influence the mean total number of bonds that at some point in time become load bearing. As our numerical results confirm, however, the bonds of deformable microvilli generally live longer, and their load-bearing stage lasts longer. A prolonged persistence of the bonds at high shear stresses was also noticed by Alon *et al.*[1] In addition, our quantitative analyses indicate that under the conditions studied the microvillus extension is a dominant component of the microvillus deformation process. The microvillus extends more and at a higher rate than the microvillus tether does. The mean force acting on the microvillus when its last bond breaks is 55 pN, exceeding the mean microvillus threshold bond force by only 7.5 pN; therefore the life of an average microvillus tether is relatively short soon after it starts developing. This could be different at higher forces imposed by higher shear stresses, which remain to be studied.

A microvillus starts to deform as soon as a bond force starts acting on it, and the deformation process continues (even when the cell seems to be at rest) as long as the force is present. This implies that even under very low shear stresses, microvillus deformation is occurring in rolling cells, although it may not be easy to observe experimentally. Our modeling demonstrates diverse microvillus deformation activities at a wall shear rate of 50 s^{-1}, whereas Schmidtke and Diamond[28] detected no tethers in their experiments at wall shear rates of 50 s^{-1} and below, presumably because of limitations in the spatial and temporal resolution of available experimental techniques.

Shao *et al.*[29] and others[6,22] propose the spring formula $F = \sigma\,[\Delta L(t)]$ to model microvillus extension in cell rolling, that is, Eq. (2) truncated (i.e., without a damper). For a given microvillus bond force F, Eq. (4) yields $F = \sigma\,[\Delta L(\infty)]$, making the truncated equation true for $t = \infty$ only. This means that the quantity $\Delta L(t)$ calculated from the truncated equation represents the approximate extension that a microvillus would reach if force F acted on it for a sufficiently long time, of the order of several seconds. Yet applying the truncated formula for every time step in a simulation (time steps can be as short as 0.1 μs, depending on shear stress) greatly overestimates microvillus extension. Shao *et al.*[29] estimate the longest possible microvillus length under quasi-steady conditions to be 285% of the microvillus equilibrium length at a wall shear rate of 22 s^{-1}. Our longest microvillus–tether complex observed during cell rolling at a wall shear rate of 50 s^{-1} is 184% of the microvillus equilibrium length.

A complete biophysical/biochemical explanation why and how a microvillus suddenly starts developing a tether when its bond force reaches a value above its threshold bond force remains to be given. It has been suggested that the threshold bond force depends on the degree of association between membrane and cytoskeleton in individual microvilli. A stronger membrane–cytoskeleton association yields a higher threshold bond force.[26,29] Formation of a tether from the cell plasma membrane involves separation of the membrane lipid bilayer from the cytoskeleton.[13] During tether elongation the cell plasma membrane flows into the growing tether.[7,12] According to the dashpot model, tether elongation starts occurring under a force

of $(F - F_0)$ [the microvillus bond force minus the microvillus threshold bond force], where $F > F_0$. In cell rolling, force F is applied to a microvillus which is already extended to a certain degree. If F^* is the last microvillus bond force extending the microvillus, then $F^* < F_0 < F$. When the tether stars developing, there is a component of force of at least $(F_0 - F^*)$ which may be needed for lipid bilayer-cytoskeleton separation when the microvillus is not fully extended. In an ideal case when force F is applied to a microvillus which is fully extended under $F^* = F_0$, that component of force is reduced to zero. Whether microvillus elongation is correlated with the lipid bilayer-cytoskeleton separation process remains open to investigation.

In summary, this work shows that microvilli modeled as Kelvin–Voigt elements with viscous tethers forming above a force threshold decrease the translational velocity of rolling leukocytes by 35%, from 3.42 to 2.23 $\mu m\ s^{-1}$, at a wall shear rate of 50 s^{-1}. The mean total number of bonds increases and the mean fraction of bonds that become load-bearing decreases, compared to the corresponding model with non-deformable microvilli. Although as a net result the mean number of load-bearing bonds remains very similar in the two cases, the mean duration of the load-bearing state for bonds of deformable microvilli increases by 54%, from 0.13 to 0.20 s. Compared to previous efforts aimed at modeling extensible microvilli, the Kevin–Voigt model more realistically matches data obtained in micropipette experiments. Conceptually, our model agrees with experimental results obtained in flow chamber studies[20] that suggest a stabilizing effect of extensible microvilli, although the experimental work was conducted at higher shear rates.

ACKNOWLEDGMENT

This work was supported by the National Institutes of Health, Grant #2R01EB002185.

REFERENCES

[1]Alon, R., D. A. Hammer, and T. A. Springer. Lifetime of P-selectin-carbohydrate bond and its response to tensile force in hydrodynamic flow. *Nature* 374:539–542, 1995.

[2]Atherton, A., and G. V. R. Born. Relationship between the velocity of rolling granulocytes and that of the blood flow in venules. *J. Physiol.* 233:157–165, 1973.

[3]Bell, G. I., M. Dembo, and P. Bongrand. Cell adhesion. Competition between nonspecific repulsion and specific bonding. *Biophys. J.* 45:1051–1064, 1984.

[4]Bell, G. I Models for the specific adhesion of cells to cells. *Science* 200:618–627, 1978.

[5]Bruehl, R. E., T. A. Springer, and D. F. Bainton. Quantitation of L-selectin distribution on human leukocyte microvilli by immunogold labeling and electron microscopy. *J. Histochem. Cytochem.* 44:835–844, 1996.

[6]Caputo, K. E., and D. A. Hammer. Effect of microvillus deformability on leukocyte adhesion explored using adhesive dynamics simulations. *Biophys. J.* 89:187–200, 2005.

[7]Dai, J., and M. P. Sheetz. Mechanical properties of neuronal growth cone membranes studied by tether formation with laser optical tweezers. *Biophys. J.* 68:988–996, 1995.

[8]Dembo, M. On peeling an adherent cell from a surface. *Lec. Math. Life Sci.* 24:51–77, 1994.

[9]Finger, E. B., R. E. Bruehl, D. F. Bainton, and T. A. Springer. A differential role for cell shape in neutrophil tethering and rolling on endothelial selectins under flow. *J. Immunol.* 157:5085–5096, 1996.

[10]Graf, C., and J. P. Barras. Rheological properties of human blood plasma—a comparison of measurements with three different viscometers. *Cell. Mol. Life Sci.* 35:224–225, 1979.

[11]Hochmuth, R. M. Micropipette aspiration of living cells. *J. Biomech.* 33:15–22, 2000.

[12]Hochmuth, R. M., J. Y. Shao, J. Dai, and M. P. Sheetz. Deformation and flow of membranes into tethers extracted from neuronal growth cones. *Biophys. J.* 70:359–369, 1996.

[13]Hwang, W. C., and R. E. Waugh. Energy of dissociation of lipid bilayer from the membrane skeleton of red blood cells. *Biophys. J.* 72:2669–2678, 1997.

[14]Khismatullin, D. B., and G. A. Truskey. Three-dimensional numerical simulation of receptor-mediated leukocyte adhesion to surfaces: effects of cell deformability and viscoelasticity. *Phys. Fluids* 17:031505.1–031505.21, 2005.

[15]Kumar, S., I. Z. Maxwell, A. Heisterkamp, T. R. Polte, T. P. Lele, M. Salanga, E. Mazur, and D. E. Ingber. Viscoelastic retraction of single living stress fibers and its impact on cell shape, cytoskeletal organization, and extracellular matrix mechanics. *Biophys. J.* 90:3762–3773, 2006.

[16]Li, F., H. P. Erickson, J. A. James, K. L. Moore, R. D. Cummings, and R. P. McEver. Visualization of P-selectin glycoprotein ligand-1 as a highly extended molecule and mapping of protein epitopes for monoclonal antibodies. *Biol. Chem.* 271:6342–6348, 1996.

[17]Mehta, P., R. D. Cummings, and R. P. McEver. Affinity and kinetic analysis of P-selectin binding to P-selectin glycoprotein ligand-1. *J. Biol. Chem.* 273:32506–32513, 1998.

[18]Moore, K. L., K. D. Patel, R. E. Bruehl, L. Fugang, D. A. Johnson, H. S. Lichenstein, R. D. Cummings, D. F. Bainton, and R. P. McEver. P-selectin glycoprotein ligand-1 mediates rolling of human neutrophils on P-selectin. *J. Cell Biol.* 128:661–671, 1995.

[19]Moore, K. L., A. Varki, and R. P. McEver. GMP-140 binds to a glycoprotein receptor on human neutrophils: evidence for a lectin-like interaction. *J. Cell Biol.* 112:491–499, 1991.

[20]Park, E. Y. H., M. J. Smith, E. S. Stropp, K. R. Snapp, J. A. DiVietro, W. F. Walker, D. W. Schmidtke, S. L. Diamond, and M. B. Lawrence. Comparison of PSGL-1 microbead and neutrophil rolling: microvillus elongation stabilizes P-selectin bond clusters. *Biophys. J.* 82:1835–1847, 2002.

[21]Patel, K. D., M. U. Nollert, and R. P. McEver. P-selectin must extend a sufficient length from the plasma membrane to mediate rolling of neutrophils. *J. Cell Biol.* 131:1893–1902, 1995.

[22]Pawar, P., S. Jadhav, C. D. Eggleton, and K. Konstantopoulos. Roles of cell and microvillus deformation and receptor-ligand binding kinetics in cell rolling. *Am. J. Physiol. Heart Circ. Physiol.* 295:H1439–H1450, 2008.

[23]Pospieszalska, M. K., A. Zarbock, J. E. Pickard, and K. Ley. Event-Tracking Model of Adhesion identifies load-bearing bonds in rolling leukocytes. *Microcirculation* 16:115–130, 2009.

[24]Ragsdale, G. K., J. Phelps, and K. Luby-Phelps. Viscoelastic response of fibroblasts to tension transmitted through adherens junctions. *Biophys. J.* 73:2798–2808, 1997.

[25]Ramachandran, V., M. Williams, T. Yago, D. W. Schmidtke, and R. P. McEver. Dynamic alterations of membrane tethers stabilize leukocyte rolling on P-selectin. *Proc. Natl. Acad. Sci.* 101:13519–13524, 2004.

[26]Raucher, D., and M. P. Sheetz. Characteristics of a membrane reservoir buffering membrane tension. *Biophys. J.* 77:1992–2002, 1999.

[27]Schmid-Schönbein, G. W. Leukocyte biophysics. An invited review. *Cell Biophys.* 17:107–135, 1990.

[28]Schmidtke, D. W., and S. L. Diamond. Direct observation of membrane tethers formed during neutrophil attachment to platelets or P-selectin under physiological flow. *J. Cell Biol.* 149:719–729, 2000.

[29]Shao, J. Y., H. P. Ting-Beall, and R. M. Hochmuth. Static and dynamic lengths of neutrophil microvilli. *Proc. Natl. Acad. Sci.* 95:6797–6802, 1998.

[30]Springer, T. A. Adhesion receptors of the immune system. *Nature* 346:425–434, 1990.

[31]Zipursky, A., E. Bow, R. S. Seshadri, and E. J. Brown. Leukocyte density and volume in normal subjects and in patients with acute lymphoblastic leukemia. *Blood* 48:361–371, 1976.